On-line separators for the Dubna Superheavy Element Factory

A.G. Popeko *

Flerov Laboratory of Nuclear Reactions, JINR, 141980 Dubna, Russia

ARTICLE INFO

ABSTRACT

The main goal of creation of a Superheavy Element Factory at the Flerov Laboratory of Nuclear Reactions (FLNR) is to sufficiently improve the efficiency of studies on heavy and superheavy nuclei. The factory will be based on a high-current DC-280 cyclotron. The use of beams with the intensity up to 6×10^{13} s^{-1} (10 pµA) requires effective separators providing high suppression of unwanted reaction products. Following the analysis of the kinematic characteristics of several hundreds of reactions, a conclusion was drawn that it is necessary to construct three separators optimized for specific tasks: a universal gas-filled separator for synthesis and study of the properties of heavy isotopes, a velocity filter for spectroscopic investigations, and a pre-separator for further chemical separation and precise mass measurements.

© 2016 Elsevier B.V. All rights reserved.

1. Introduction

The production cross sections of superheavy elements (SHE) with $Z = 112$–118 in ^{48}Ca-induced fusion reactions with actinide targets are in the range of a few picobarns or less (1 event/month–1 event/week) [1]. To carry out further studies of SHE, a significant increase in the overall experiment efficiency is needed. The use of a new experimental complex "Superheavy Element Factory" will increase the production rate of SHE by a factor of 10 or more.

The heaviest isotope from which a target for SHE synthesis can be manufactured is ^{251}Cf; thus, to get access to elements with higher Z, one needs to use beams of ^{50}Ti, ^{54}Cr, ^{58}Fe, etc. Symmetric fusion reactions, like ^{136}Xe + ^{138}Ba, and ^{150}Nd + ^{150}Nd, and transfer reactions, like ^{136}Xe + ^{208}Pb and U + U, are of interest but have been insufficiently explored.

The new experimental FLNR complex will be based on a high-current DC-280 cyclotron capable of producing beams of accelerated ions with A⩽238, E⩽10 MeV/A, and with the intensity $I \leqslant 10$ pµA of ions with A⩽100 [2].

Hence, the requirements for a separator can be defined as follows:

- to separate products of reactions in a broad range of mass asymmetry in the entrance channel;

- to accept beams of accelerated ions with the intensity up to 10 pµA;
- to separate effectively products from thick ~0.5 mg/cm^2 targets;
- to provide sufficient suppression of unwanted reaction products.

2. What and from what to separate?

Using the modern technique, it is possible to study products of fusion reactions of massive nuclei with cross sections >20 fb [3] (1 fb = 10^{-39} cm^2). The desired products must be separated from the undesired ones, which have higher yields up to 10^{15}. We need to suppress:

- unreacted full-energy primary beam particles and projectile-like reaction products;
- elastically knocked-out target atoms and target-like reaction products; this process has a cross section of ≈1 b, and the flux of such particles can exceed 10^6–10^7 s^{-1};
- scattered beam particles; the flux of these particles depends mostly on the quality of beam transportation and can be significantly reduced by correctly tuning an accelerator and a beam line;
- neutrons and γ-quanta; this background can be lowered by an appropriate shielding, especially of a beam dump, and by preventing focal plane detectors from directly facing the target;

* Tel.: +7 496 2162146.
E-mail address: popeko@jinr.ru

- products of reactions of a beam with secondary components of targets (N, O, S), target backings (Be, Al, Ti, Zr), target holders, supporting grids, cowering layers, collimators, etc.; one must pay special attention to the choice of materials to avoid interferences;
- high-energy protons and α-particles originating due to scattering of primary beam on a filling gas, which is hydrogen or helium in gas-filled devices.

3. Energy, angular, and charge distributions of evaporation residues

If an accelerated projectile and a target nucleus form a compound nucleus (CN), the latter obtains a linear momentum of the beam particle. The CN de-excites by evaporation of neutrons, protons, α-particles or γ-quanta, forming an evaporation residue (ER). Whereas the emission of particles changes the momentum of ERs only slightly, the slowdown and multiple scattering essentially affect energy and angular distributions of ERs emerging from different depths of a target.

The well-known computer code SRIM [4] describes ions with $Z \leqslant 92$ and cannot be applied either to actinide targets or to SHE. For our purposes, we developed a special full Monte-Carlo code [5] that allows simulation of angular and energy distributions of EVRs. The code [5] also generates an input for another ion optical program [6] designed for tuning a separator and estimating transmission and yield of the desired reaction products.

For a more detailed analysis, the data on the ionic charge distribution characteristics are necessary. At final stages of the de-excitation, ERs emit Auger-electrons, which make the charge distribution unpredictable. Passing of ERs through a thin carbon foil placed at certain distance downstream the target, equilibrates the charges of ions according to their velocity.

The charge systematics [7] has been found the most appropriate to describe the passage of heavy and superheavy nuclei stripped on carbon foils through vacuum separators [8,9]. For the description of beam particles, the formula from [10] is widely used. Symmetric charge distributions fit well within the Gaussian law.

In regard to gas-filled separators, the systematics applicable for hydrogen and helium filling was proposed in [11]. The average charges of actinide and superheavy ions, moving in hydrogen at a pressure of about 1 mbar and with a precision of about 4%, can be determined as proposed in [12], and the average charges of those moving through rarified helium can be determined as specified in [13]. The global fit to the experimentally measured average charges of heavy ions in He, considering the influence of the electronic structure, is presented in [14]. For the description of asymmetric charge distributions, the chi-squared law (χ_ν^2) can be used, as proposed in [15].

4. Separator efficiency

When characterizing a separator, one often uses its resolution or/and transmission of the desired reaction products. These characteristics are insufficient in our case because for very thin targets, one can reach very high resolving power and transportation efficiency close to 1, but at a vanishing counting rate at the exit of the set-up. When increasing the target thickness, one introduces higher angular and energy scattering; the transmission decreases, but the production rate grows. For thick targets, one must also take into account the dependence of the cross section on the beam energy.

A more detailed analysis performed using the code [6] showed that the counting rate at the exit of the set-up (being proportional to the product of the target thickness and transmission) grows and reaches saturation at a certain target thickness. The simulated yield of ^{288}Fl produced in the reaction ^{48}Ca(235 MeV) + ^{244}Pu(PuO$_2$) $\rightarrow$ ^{288}Fl + 4n passed through the existing Dubna Gas-Filled Recoil Separator (DGFRS) [1] as a function of the ^{244}PuO$_2$ target thickness is presented in Fig. 4 (lower curve, circles).

The optimal target thickness depends on the reacting partners, reaction characteristics, energy of the bombarding particles, composition of the target, and on angular, energy, and charge acceptances of the used device. The targets commonly used at the existing on-line separators have thicknesses within the range 0.3–0.5 mg/cm^2, which covers only 10–20% of the excitation functions. The specific requirements for the development of targets for synthesis of superheavy elements were considered in [16].

5. How to separate?

On-line spatial separation can be accomplished in magnetic and electric fields owing to the differences in magnetic rigidities $B \times \rho$ (magnetic analyzers), electric rigidities E/q (separators with static or pulsed electric fields), and velocities of ions (velocity filters).

The kinematic characteristics for several reactions – the energies of particles, the magnetic rigidities of particles moving in vacuum after stripping on a carbon foil, those moving in helium and in hydrogen, the velocities and the electric rigidities in vacuum – are presented in Table 1.

The energy of the elastically scattered H ions (protons) is in the range of 15–20 MeV and that of the He ions (α-particles) is within the range 55–70 MeV.

From Table 1, one can conclude that it is impossible to separate reaction products in vacuum using only magnetic fields, since the magnetic rigidities of the reaction partners overlap sufficiently (see Fig. 1). This is the case for the reactions at the Coulomb barrier when the ERs are not fully stripped.

The next conclusions are:

- use of electrostatic separators and velocity filters is always possible;
- a separator filled with He cannot satisfactory separate products of asymmetric reactions, e.g., the evaporation residues ^{255}No from the target-like reaction products – ^{238}U;
- use of gas-filled separators is impossible in the case of symmetric reactions;
- a separator filled with H$_2$ provides better separation than that filled with He [17], but higher magnetic fields are needed; besides, H$_2$ is flammable.

The performed analysis allows one to define the critical requirements for the dispersive elements of set-ups used in studies of

Table 1
The kinematic characteristics of reaction products.

Ion	Energy (MeV)	$B \times \rho$ (vac) T × m	$B \times \rho$ (He) T × m	$B \times \rho$ (H$_2$) T × m	velocity (cm/ns)	E/q_{vac} (MV)
$^{22}Ne + ^{238}U \rightarrow ^{260}No^*$						
^{22}Ne	112.5	0.76	0.76	0.76	3.14	11.7
^{260}No	9.5	0.74	1.82	2.45	0.26	0.99
^{238}U	34.8	0.72	1.89	2.01	0.53	1.93
$^{48}Ca + ^{244}Pu \rightarrow ^{292}Fl^*$						
^{48}Ca	236	0.88	0.94	0.94	3.1	13.0
^{292}Fl	38.8	0.79	2.0	2.18	0.51	2.0
^{244}Pu	129.7	0.83	1.65	1.49	1.0	4.2
$^{136}Xe + ^{136}Xe \rightarrow ^{272}Hs^*$						
^{136}Xe	600	1.10	1.38	1.38	3.0	15.7
^{272}Hs	300	0.95	1.39	1.21	1.46	6.85
^{136}Xe	600	1.10	1.38	1.38	3.0	15.7
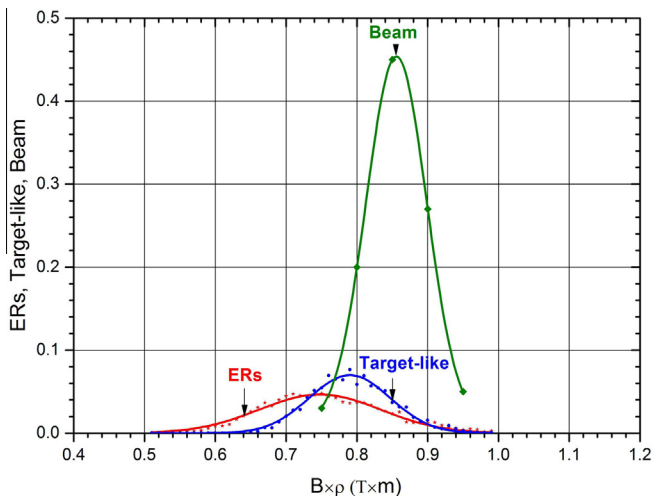
Fig. 1. Distributions of magnetic rigidities of the $^{48}Ca + ^{244}Pu \rightarrow ^{288}Fl + 4n$ reaction products.

heavy nuclei. A vacuum separator must be able to transport particles with the electric rigidity up to 10 MV and the magnetic rigidity up to 1 T × m. Gas-filled devices must be designed for particles with the magnetic rigidity up to 3.0 T × m.

6. Choice of a separator

Three different separators are underway to address the unique needs of experiments planned at the SHE Factory:

- a gas-filled separator for experiments on the synthesis and study of superheavy elements;
- a velocity filter as the most suitable device for studying the spectroscopic properties of heavy nuclei and for investigating the reaction mechanisms leading to the formation of the heaviest and exotic isotopes;
- a simplified version of a gas-filled separator that will serve as a pre-separator for primary beam suppression and can be used to study the chemical properties of the heaviest elements and precise mass measurements.

7. Principle of operation of a gas-filled separator

Owning to multiple charge-changing interactions, ions move through a gas-filled separator with an average charge $\langle q \rangle$. The distinctive feature of charge-changing collisions is that $\langle q \rangle$ is approximately proportional to the ion velocity. This peculiarity leads to effective charge and energy focusing.

The advantages of gas-filled separators are: high-efficient transportation of complete fusion reaction products, the ability to accept high-beam currents due to cooling of a target by a filling gas, simplicity, and relatively low costs.

The main disadvantage of the gas-filled separator is its limited applicability: it cannot be used in research with symmetric reactions. Filling gas causes additional disadvantages: elastically scattered long-range protons and α-s, impossibility of using MCPs in ToF-measurements, a necessity for an entrance window or differential pumping.

Table 2 summarizes the data on the known gas-filled electromagnetic on-line separators used for synthesis and investigations of heavy isotopes. In the description of the configuration, D stands for dipole and D_h for horizontally focusing dipole magnets, Q_h and

Table 2
Data on the known gas-filled electromagnetic on-line separators.

Set-up	DGFRS	GARIS	RITU	BGS	TASCA	SHANS
Configuration	DQ_hQ_v	DQ_hQ_vD	$Q_vDQ_hQ_v$	Q_vD_hD	DQ_hQ_v	$Q_vD_hQ_vQ_h$
Deflection angle	23°	(45 + 10)°	25°	70°	30°	52°
$B \times \rho$ (max, T × m)	3.1	2.15	2.2	2.5	2.4	2.9
Dispersion (mm/%B × ρ)	7.5	9.7	10.0	20.0	9.0	7.3
Length (m)	4.0	5.75	4.7	4.6	3.5	6.5
Reference	[1]	[18]	[19]	[20]	[21]	[22]

Q_v are horizontally and vertically focusing quadrupole magnets, respectively.

Over the past 15 years, six new elements with Z = 113–118 and about 50 heaviest isotopes have been discovered [1] at DGFRS, which was developed at the end of 1980s [23].

As part of the project on the upgrade of the accelerator complex of the Flerov Laboratory, it is planned to construct a next-generation set-up "DGFRS-II".

8. A new gas-filled separator DGFRS-II

To understand the factors causing losses of EVRs during their passage through a gas-filled separator, we performed computer simulation of their trajectories in DGFRS [1]. This set-up comprises a DQ_hQ_v scheme. The gap in the dipole magnet D is 60 mm, the diameter of the aperture of the Q1 and Q2 quadrupoles is 200 mm, and their length is 370 mm. The results of simulation are shown in Fig. 2.

As one can see from the figure, most losses of ERs occur in the dipole magnet. This is obvious because it is quite difficult to construct a magnet with a large gap and a strong (1.7 T) homogeneous field. The transmission can be improved by setting a quadrupole in front of the dipole magnet and by increasing its gap. The new gas-filled separator will comprise the $Q_vD_hQ_vQ_hD$ ion optical scheme. A similar schematic has the gas-filled separator GARIS-II [24].

The quadrupole Q1 focuses EVRs in the vertical direction. The dipole magnet D30 with a deflection angle of 30° and a gap of 120 mm focuses the particles by the rotated rear pole face in the horizontal direction. The Q2 and Q3 quadrupoles focus ERs on the focal plane detector. The dipole D10 with a deflection angle of 10° and a gap of 120 mm reduces the background from the elastically scattered gas atoms, i.e., hydrogen (protons) or helium (α-particles).
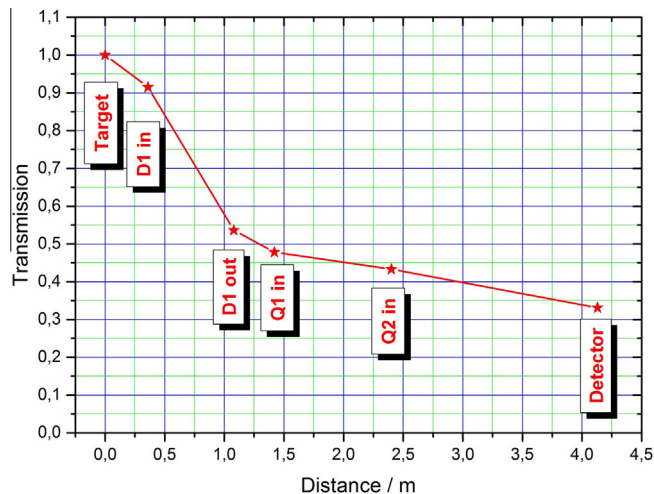
Fig. 2. The distribution of losses of ERs passing through the DQQ separator.
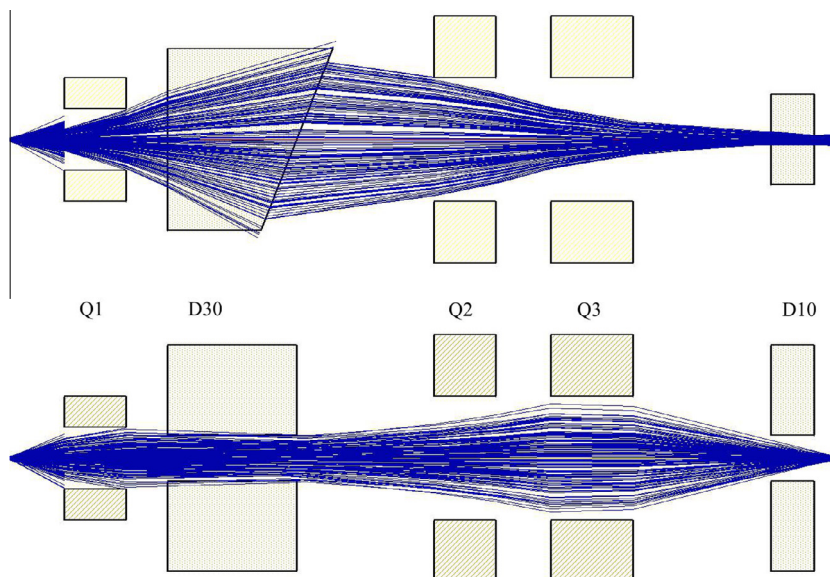
Fig. 3. Simulated trajectories of ^{288}Fl ions passing through the new gas-filled separator DGFRS-II. The field gradients in quadrupoles are GQ1 = 10.67 T/m, GQ2 = 1.89 T/m, and GQ3 = 4.50 T/m, the total length is 6.3 m.

The simulated trajectories of ^{288}Fl ions, produced in the ^{48}Ca(235 MeV) + ^{244}Pu(0.6 mg/cm^2 PuO^2) $\rightarrow$ ^{288}Fl + 4n reaction and passing through the new gas-filled separator, are shown in Fig. 3.

The characteristics of the principal components of DGFRS-II are presented in Table 3.

The ion-optical calculations and modeling showed (see Fig. 4, upper curve, stars) that the overall efficiency of the QDQQD gas-filled separator is expected to be higher by a factor of 3 in comparison to that of the existing DQQ set-up.

9. Separator for Heavy ELement Spectroscopy: velocity filter SHELS

Velocity filters perform charge-independent focusing, and their efficiency is a bit lower than that of gas-filled set-ups. However, velocity filters can be applied in studies of reactions independent of their asymmetry.

The velocity filter called "SHELS" was developed as a result of reconstruction of the VASSILISSA electrostatic separator [9]. The goals of the upgrade were to increase the transmission of products of asymmetric reactions and to extend the region of the reactions to be investigated up to symmetric combinations. The detailed description of SHELS is presented in a special report to this conference [25] (see: A.G. Popeko et al., "Separator for Heavy ELement Spectroscopy – velocity filter SHELS").

The new separator is composed of two identical mirror symmetric velocity filters with static, spatially separated electric and magnetic fields. Its ion optical scheme can be described as MQ-MQ-MQ-ES-MS-MS-ES-MQ-MQ-MQ-MS, where MQ denotes Magnetic Quadrupole lenses, ES are Electrostatic Sector fields (deflectors), and MS stands for Magnetic Sector fields. A general view of SHELS during assembly is shown in Fig. 5.

Each filter consists of a parallel, flat plate condenser and a dipole magnet. The condensers are designed in such a way as to

Table 3
Principal components of DGFRS-II.

Quadrupole magnet Q1	
Maximum field gradient	13.3 T/m
Magnetic length	0.45 m
Bore diameter	0.15 m
Quadrupole magnets Q2, Q3	
Maximum field gradient	6.0 T/m
Magnetic length	0.60 m
Bore diameter	0.30 m
Magnetic sector D30	
Bending radius	1.8 m
Nominal deflection angle	30°
Front/rear pole face angle	0/−50°
Maximum field strength	1.8 T
Gap height	0.12 m
Magnetic sector D10	
Bending radius	1.8 m
Nominal deflection angle	10°
Front/rear pole face angle	0/+10°
Maximum field strength	1.8 T
Gap height	0.12 m

Fig. 4. Simulated yields of Fl plotted as functions of the PuO$_2$ target thickness for the DQQ set-up (lower curve, circles) and for the QDQQD set-up (upper curve, stars).

Fig. 5. General view of the velocity filter SHELS.

allow change of distance between their plates from 10 to 20 cm. This is done for optimal matching of angular distribution and the electric rigidity of particles and makes accessible ERs with an electric rigidity up to 10 MV. The focusing system of SHELS consists of two magnetic quadrupole triplets. The last dipole magnet with a deflection angle of $\approx 8°$ prevents focal plane detectors from directly facing the target.

For the first trial, a ^{22}Ne beam from the U-400 cyclotron was delivered to SHELS in May 2013 [26]. The ERs from the reactions ^{197}Au(^{22}Ne,4–6n)$^{213-215}$Ac and ^{198}Pt(^{22}Ne,5–7n)$^{213-215}$Ra were detected. The results of measurements agree well with the expected ones. The suppression factor of the primary full-energy beam was found to be better than 5×10^{15} and depends mostly on the accelerator and beam line tuning. The evaluation of other characteristics needs further measurements.

10. Pre-separator

Some of the newly discovered superheavy isotopes have half-lives ranging from seconds to ≈ 1d [1], times – reachable by radiochemical off-line methods. The advantages of these methods were demonstrated in the experiments on the synthesis of element 115 in the ^{243}Am(^{48}Ca,3n) reaction [27]. Three decays of the long-lived isotope ^{268}Db – a descendent of element 115 – were detected on-line at DGFRS after collection a beam dose of 4.3×10^{18}. Whereas following off-line chemical isolation of elements belonging to the fifth group, including dubnium, from a catcher, placed behind the target, 15 events were detected at a total beam dose of 3.4×10^{18}. The fivefold gain factor is caused by the use of a thicker 1.2-mg/cm^2 target and by higher efficiency of separation.

The evacuation of reaction products stopped in a gas media by means of electric fields (gas catcher) makes available for precise mass measurements reaction products with half-lives >0.02 s [28]. A gas jet transportation from a Recoil Transfer Chamber allows one spectroscopic [29] or chemical studies of reaction products with half-lives >1 s [30,31].

The limitations of radiochemical techniques are caused by the necessity to position the collection area adjacent to the target. Most of the problems can be solved by introducing between the target and stopping media a pre-separator, which rejects the primary beam and target-like reaction products. The requirements for this device are not as strict as those for on-line separators as long as following devices perform definitive separation. Therefore we consider a simplified gas-filled separator with the reduced down to 20° deflection angle, as a pre-separator. A possible
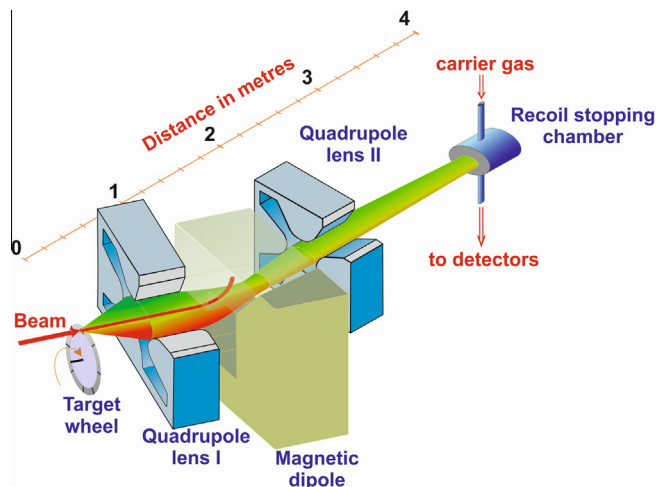
Fig. 6. The layout of the $Q_v DQ_h$ pre-separator.

lay-out of a pre-separator comprising a $Q_v DQ_h$ ion optical scheme, is shown in Fig. 6.

The performed analysis shows that the transmission of ^{288}Fl, produced in the reaction of ^{48}Ca with a 1.0-mg/cm^2 ^{244}PuO$_2$ target, can reach 60–65%. The construction of a preseparator based on a superconducting double focusing magnet is under discussion.

11. Conclusion

- The new velocity filter SHELS is currently in test operation and is basically ready for experiments.
- The universal QDQQD gas-filled separator is prepared for manufacture.
- The gas-filled pre-separator project is in progress.

References

[1] Yu. Oganessian, J. Phys. G: Nucl. Part. Phys. 34 (2007) R165.
[2] A.G. Popeko, S.N. Dmitriev, G.G. Gulbekian, M.G. Itkis, Yu.Ts. Oganessian, in: Proc. of the First African Symp. on Exotic Nuclei, Cape Town, South Africa, 2–6 Dec 2013, World Sci. Publ. Co., 2015, p. 91.
[3] K. Morita, K. Moritomo, D. Kaji, H. Haba, K. Ozeki, Y. Kudou, T. Sumita, Ya. Wakabayashi, A. Yoneda, K. Tanaka, S. Yamaki, R. Sakai, T. Akiyama, Sh. Goto, H. Hasebe, M. Huang, T. Huang, E. Ideguchi, Yo. Kasamatsu, K. Katori, Yo. Kariya, H. Kikunaga, H. Koura, H. Kudo, A. Mashiko, K. Mayama, Sh. Mitsuo, T. Moriya,

M. Murakami, H. Murayama, S. Namai, A. Ozawa, N. Sato, K. Sueki, M. Takeyama, F. Tokani, A. Yoshida, J. Phys. Soc. Japan 81 (2012) 103201.

[4] J. Ziegler, SRIM/TRIM. <http://www.srim.org>.

[5] A.G. Popeko, O.N. Malyshev, R.N. Sagaidak, A.V. Yeremin, Nucl. Instr. Methods Phys. Res. B 126 (1997) 294.

[6] A.G. Popeko, O.N. Malyshev, A.V. Yeremin, S. Hofmann, Nucl. Instr. Methods Phys. Res. A 427 (1999) 166.

[7] V.S. Nikolaev, I.S. Dmitriev, Phys. Lett. A 28 (1968) 277.

[8] G. Münzenberg, W. Faust, S. Hofmann, P. Armbruster, K. Güttner, H. Ewald, Nucl. Instr. Methods 161 (1979) 65.

[9] A.V. Yeremin, A.N. Andreyev, D.D. Bogdanov, G.M. Ter-Akopian, V.I. Chepigin, V.A. Gorshkov, A.P. Kabachenko, O.N. Malyshev, A.G. Popeko, R.N. Sagaidak, Š. Šháro, E.N. Voronkov, A.V. Taranenko, A.Yu. Lavrentjev, Nucl. Instr. Methods Phys. Res. A 350 (1994) 608.

[10] Y. Kanai, Y. Awaya, T. Kambara, M. Kase, H.KumagaiT. Mizogawa, K. Shima, Nucl. Instr. Methods Phys. Res. A 262 (1987) 128.

[11] Yu.Ts. Oganessian, Yu.V. Lobanov, A.G. Popeko, F. Sh Abdullin, Yu.P. Kharitonov, A.A. Ledovskoy, Yu.S. Tsyganov, Z. Phys. D 21 (1991) 357.

[12] Yu.Ts. Oganessian, V.K. Utyonkov, Yu.V. Lobanov, F.Sh. Abdullin, A.N. Polyakov, I.V. Shirokovsky, Yu.S. Tsyganov, A.N. Mezentsev, S. Iliev, V.G. Subbotin, A.M. Sukhov, G.V. Buklanov, K. Subotic, Yu.A. Lazarev, K.J. Moody, J.F. Wild, N.J. Stoyer, M.A. Stoyer, R.W. Lougheed, C.A. Laue, Phys. Rev. C. 64 (2001) 064309.

[13] J. Khuyagbaatar, V.P. Shevelko, A. Borschevsky, Ch.E. Dúllmann, I.Yu. Tolstikhina, A. Yakushev, Phys. Rev. A. 88 (2013) 042703.

[14] K.E. Gregorich, Nucl. Instr. Methods Phys. Res. A 711 (2013) 47.

[15] Y. Baudinet-Robinet, P.D. Dumont, H.P. Garnir, J. Phys. B: Atom. Molec. Phys. 11 (1978) 1291.

[16] S.N. Dmitriev, A.G. Popeko, J. Radioanal. Nucl. Chem. 305 (2015) 927.

[17] Yu.Ts. Oganessian, Yu.V. Lobanov, A.G. Popeko, F.Sh. Abdullin, G.G. Gulbekian, Yu.P. Kharitonov, A.A. Ledovskoy, S.P. Tretyakova, Yu.S. Tsyganov, V.E. Zhuchko, Inst. Phys. Conf. Ser. 132 (1993) 429.

[18] K. Morita, A. Yoshida, T.T. Inamura, M. Koizumi, T. Nomura, M. Fujicka, T. Shinozuka, H. Miyatake, K. Sueki, H. Kudo, Y. Nagai, T. Toriyama, K. Yoshimura, Y. Hatsukava, Nucl. Instr. Methods Phys. Res. B. 70 (1992) 220.

[19] M. Leino, J. Äystö, T. Enqvist, P. Heikkinen, A. Jokinen, M. Nurmia, A. Ostrowski, W.H. Trzaska, J. Uusitalo, K. Eskola, P. Armbruster, V. Ninov, Nucl. Instr. Methods Phys. Res. B. 99 (1995) 653.

[20] V. Ninov, K.E. Gregorich, AIP Conf. Proc., vol. 455, AIP, Woodbury, 1998, p. 704.

[21] A. Semchenkov, W. Brüchle, E. Jäger, E. Schimpf, M. Schädel, C. Mühle, F. Klos, A. Türler, A. Yakushev, A. Belov, T. Belyakova, M. Kaparkova, V. Kukhtin, E. Lamzin, S. Sytchevsky, Nucl. Instr. Methods Phys. Res. B. 266 (2008) 4153.

[22] Z.Y. Zhang, L. Ma, Z.G. Gan, M.H. Huang, T.H. Huang, G.S. Li, X.L. Wu, G.B. Jia, L. Yu, H.B. Yang, Z.Y. Sun, X.H. Zhou, H.S. Xu, W.L. Zhan, Nucl. Instr. Methods Phys. Res. B. 317 (2013) 315.

[23] Yu.Ts. Oganessian, Yu.V. Lobanov, A.G. Popeko, J. Rigol, F.Sh. Abdullin, V.V. Bekhterev, G.G. Gulbekian, A.A. Ledovskoj, V.N. Melnikov, S.P. Tretjakova, Yu.P. Kharitonov, Yu.S. Tsyganov, V.A. Chugreev, in: Proc. of School-Seminar on Heavy Ion Phys., Dubna, 3–12 October, 1989, JINR, D7-90-142, p. 44.

[24] D. Kaji, K. Morimoto, N. Sato, A. Yoneda, K. Morita, Nucl. Instr. Methods Phys. Res. B 317 (2013) 311.

[25] A.G. Popeko, A.V. Yeremin, O.N. Malyshev, V.I. Chepigin, A.V. Isaev, Yu.A. Popov, A.I. Svirikhin, K. Haushild, A. Lopez-Martens, K. Rezynkina, O. Dorvaux, Nucl. Instr. Methods Phys. Res. B 376 (2016) 140.

[26] K. Rezynkina, K. Hauschild, A. Lopez-Martens, O. Dorvaux, B. Gall, F. Déchery, H. Faure, A.V. Yeremin, M.L. Chelnokov, V.I. Chepigin, A.V. Isaev, I.N. Izosimov, D.E. Katrasev, A.N. Kuznetsov, A.A. Kuznetsova, O.N. Malyshev, A.G. Popeko, Yu. A. Popov, E.A. Sokol, A.I. Svirikhin, Acta Phys. Polonica B 46 (2015) 623.

[27] Yu.Ts. Oganessian, V.K. Utyonkov, S.N. Dmitriev, Yu.V. Lobanov, M.G. Itkis, A.N. Polyakov, Yu.S. Tsyganov, A.N. Mezentsev, A.V. Yeremin, A.A. Voinov, E.A. Sokol, G.G. Gulbekian, S.L. Bogomolov, S. Iliev, V.G. Subbotin, A.M. Sukhov, G.V. Buklanov, S.V. Shishkin, V.I. Chepigin, G.K. Vostokin, N.V. Aksenov, M. Hussonnois, K. Subotic, V.I. Zagrebaev, K.J. Moody, J.B. Patin, J.F. Wild, M.A. Stoyer, N.J. Stoyer, D.A. Shaughnessy, J.M. Kenneally, P.A. Wilk, R.W. Lougheed, H.W. Gäggeler, D. Schumann, H. Bruchertseifer, R. Eichler, Phys. Rev. C. 72 (2005) 034611.

[28] M. Block, D. Ackermann, K. Blaum, C. Droese, M. Dworschak, S. Eliseev, T. Fleckenstein, E. Haettner, F. Herfurth, F.P. Heberger, S. Hofmann, J. Ketelaer, J. Ketter, H.J. Kluge, G. Marx, M. Mazzocco, Yu.N. Novikov, W.R. Plass, A. Popeko, S. Rahaman, D. Rodŕguez, C. Scheidenberger, L. Schweikhard, P.G. Thirolf, G.K. Vorobyev, C. Weber, Nature 463 (2010) 785.

[29] D. Kaji, K. Morimoto, H. Haba, E. Ideguchi, H. Koura, K. Morita, J. Phys. Soc. Japan 85 (2016) 015002.

[30] Ch.E. Dúllmann, C.M. Folden, K.E. Gregorich, D.C. Hoffman, D. Leitner, G.K. Pang, R. Sudowe, P.M. Zielinski, H. Nitsche, Nucl. Instr. Methods Phys. Res. A. 551 (2005) 528.

[31] D. Wittwer, F.Sh. Abdullin, N.V. Aksenov, Yu.V. Albin, G.A. Bozhikov, S.N. Dmitriev, R. Dressler, R. Eichler, H.W. Gäggeler, R.A. Henderson, S. Hübener, J. M. Kenneally, V.Ya. Lebedev, Yu.V. Lobanov, K.J. Moody, Yu.Ts. Oganessian, O.V. Petrushkin, A.N. Polyakov, D. Piguet, P. Rasmussen, R.N. Sagaidak, A. Serov, I.V. Shirokovsky, D.A. Shaughnessy, S.V. Shishkin, A.M. Sukhov, M.A. Stoyer, N.J. Stoyer, E.E. Tereshatov, Yu.S. Tsyganov, V.K. Utyonkov, G.K. Vostokin, M. Wegrzecki, P.A. Wilk, Nucl. Instr. Methods Phys. Res. B. 268 (2010) 28.